

Experiments with Tidal Analysis of CryoSat-2 Altimetry in the Weddell Sea and on Adjoining Ice Shelves

Edward D. Zaron, Department of Civil & Environmental Engineering, Portland State University

Summary

- Tidal aliasing properties of the CryoSat-2 orbit have been analyzed, accounting for exact-repeat, near-repeat, and crossover periodicities as a function of spatial scale.
- With enough spatial averaging, the 8 largest tides, M_2 , S_2 , N_2 , K_2 , K_1 , O_1 , P_1 , and Q_1 , can be identified and mapped.
- A spatially-coupled harmonic analysis is used here, which combines harmonic time dependence with linear spatial dependence within a local tangent plane. The size of the tangent plane varies with latitude, from about 80km to 250km.
- Because of its high inclination, the CryoSat-2 orbit plane precesses slowly, and determinations of the K_1 and K_2 tides are less accurate.
- The largest source of “noise” in the tidal analysis is the small-scale variability of the mean ice surface, which must be estimated at scales much smaller than the tides.
- Tides inferred from CryoSat-2 are compared with tides from in situ GPS and bottom pressure recorders (King et al, 2011, and Padman’s Antarctic Tide Database). CryoSat-2 tides agree with in situ measurements better than existing data-assimilative models for M_2 and S_2 , and, except for K_2 , their accuracy is similar to the data-assimilative models for the smaller tides.

Temporal Aliasing: Tidal Phase Sampling as a Function of Spatial Scale

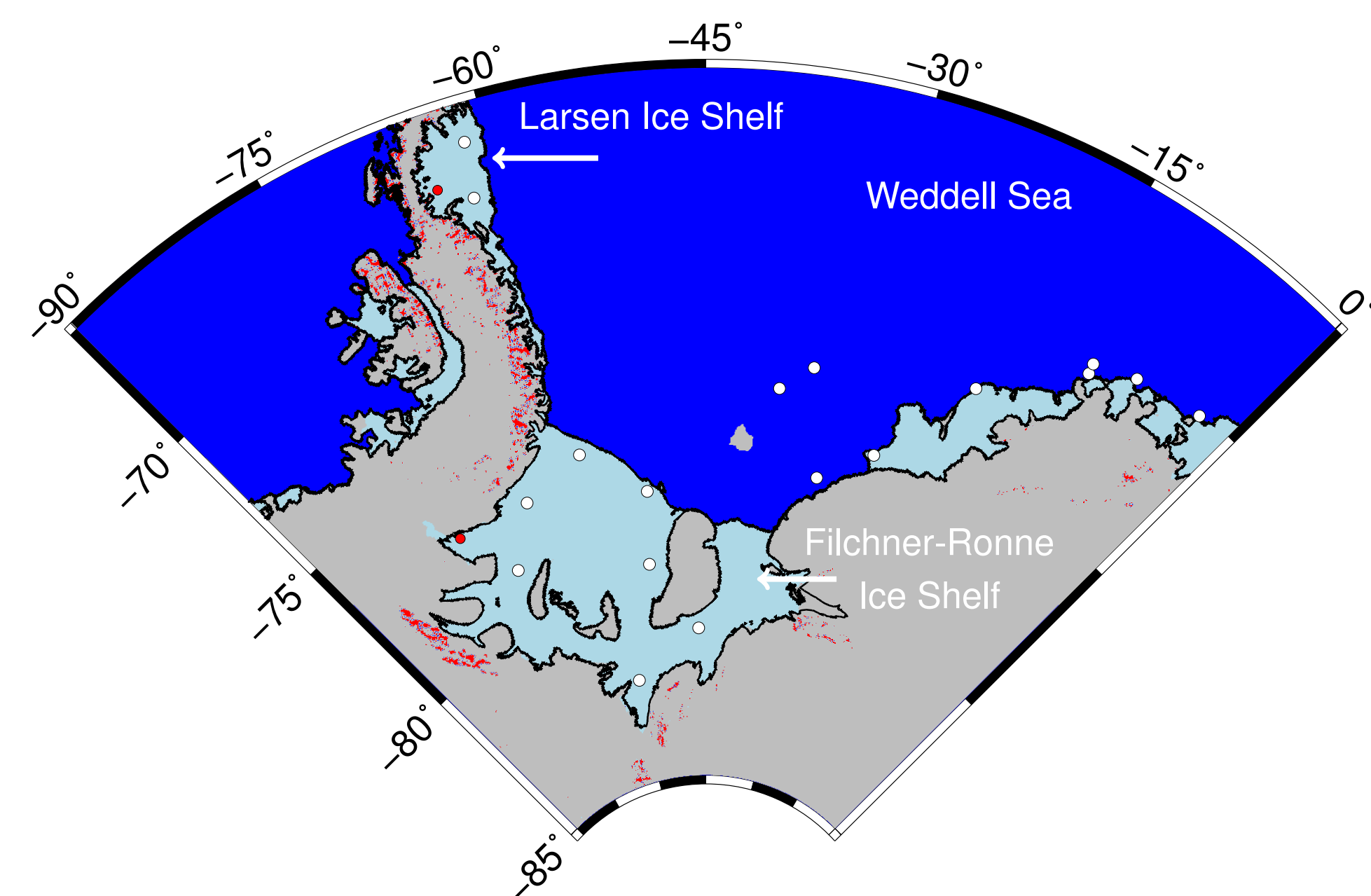


Figure 1: Analysis domain. White circles indicate locations of GPS (King et al, 2011) and bottom pressure data (Padman’s Antarctic Tide Database) used for model validation.

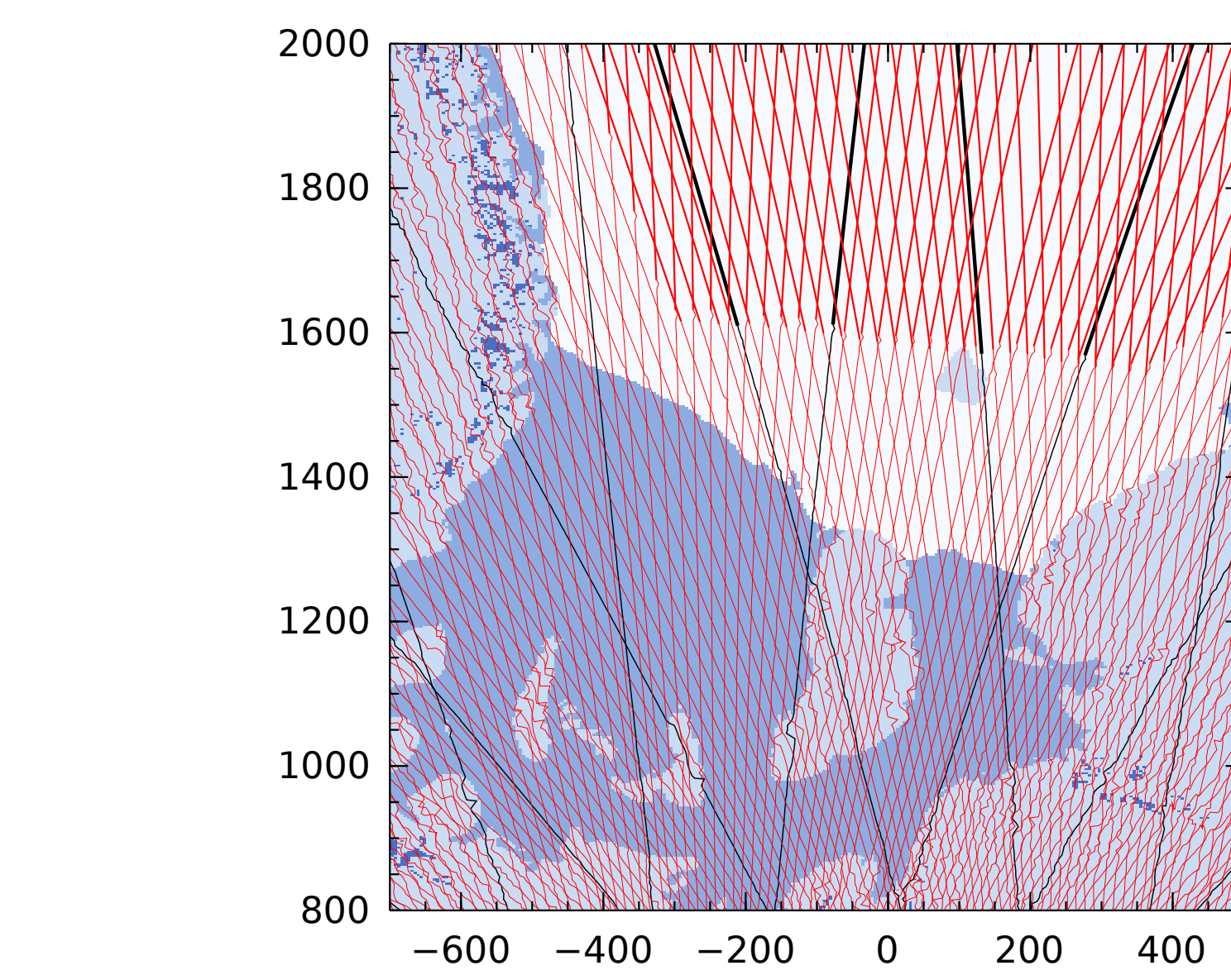


Figure 2: CryoSat-2 ground tracks during a 30-day period (polar stereographic projection with easting and northing indicated in units of km). Black lines indicate tracks within a 3-day pseudo-subcycle.

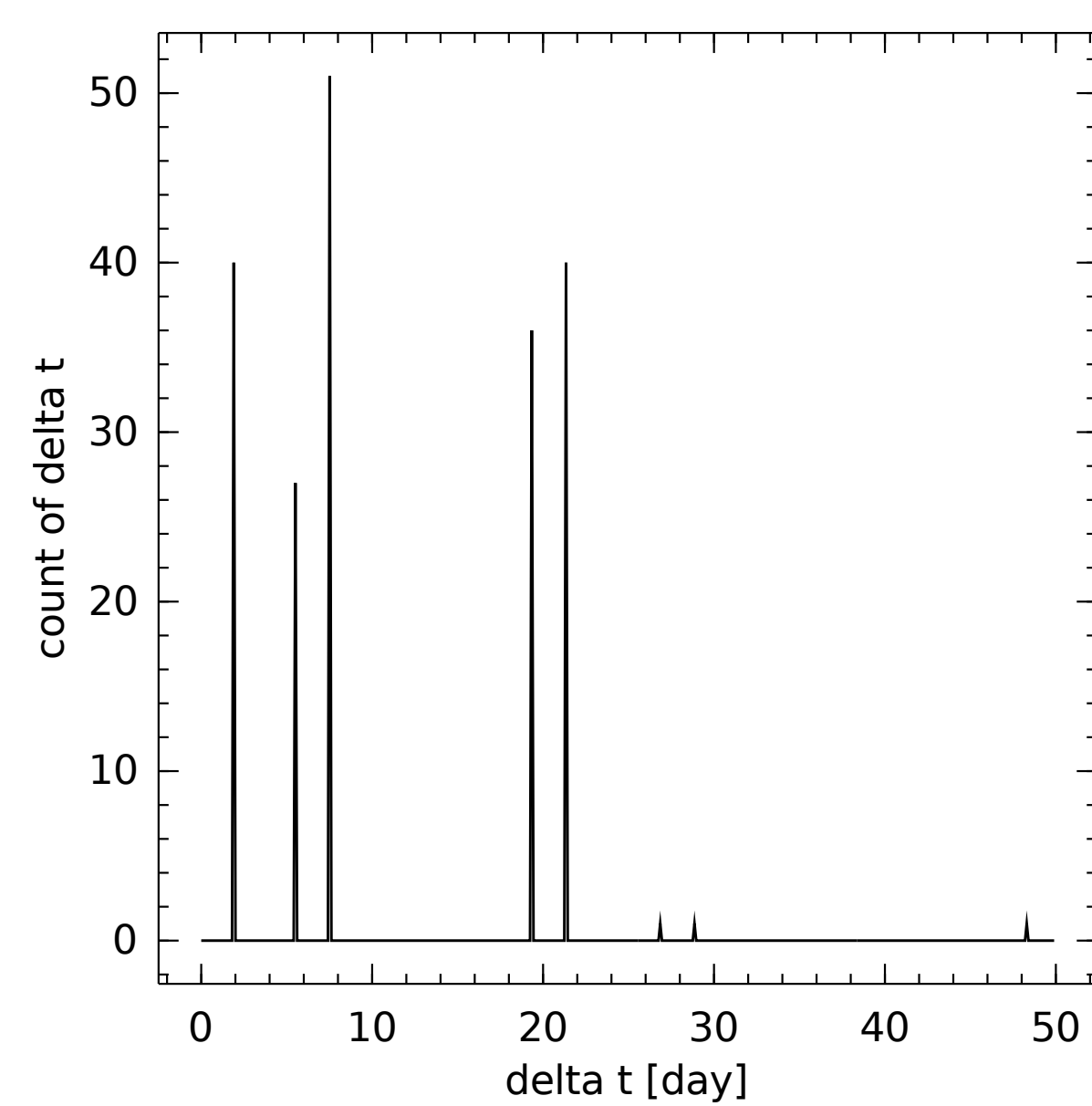


Figure 3: Histogram of sample interval for CryoSat-2 data within a 30 km-diameter disc at 70°S. Samples near $\Delta t = 2$ days and $\Delta t = 29$ days are associated with pseudo-subcycles. Samples near $\Delta t = 6$ days and $\Delta t = 20$ days are associated with intersecting ascending and descending tracks.

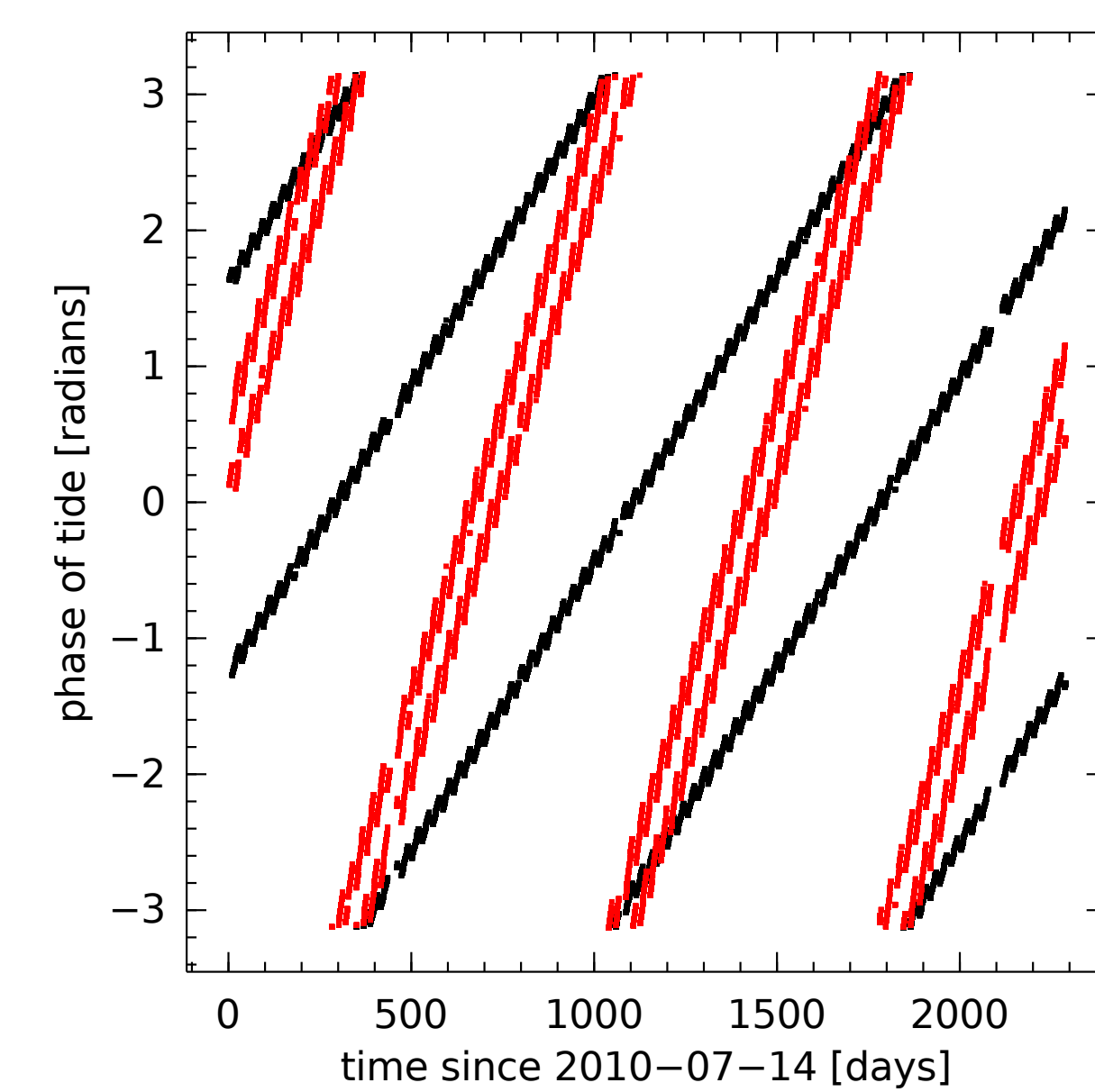


Figure 4: Phases of K_1 (black) and K_2 (red) sampled by CryoSat-2 within a 240 km \times 30 km zonal patch in the Weddell Sea. Although the alias period of K_2 is shorter than the alias period of K_1 , CryoSat-2 frequently samples the K_1 tide at two phases almost 180° apart.

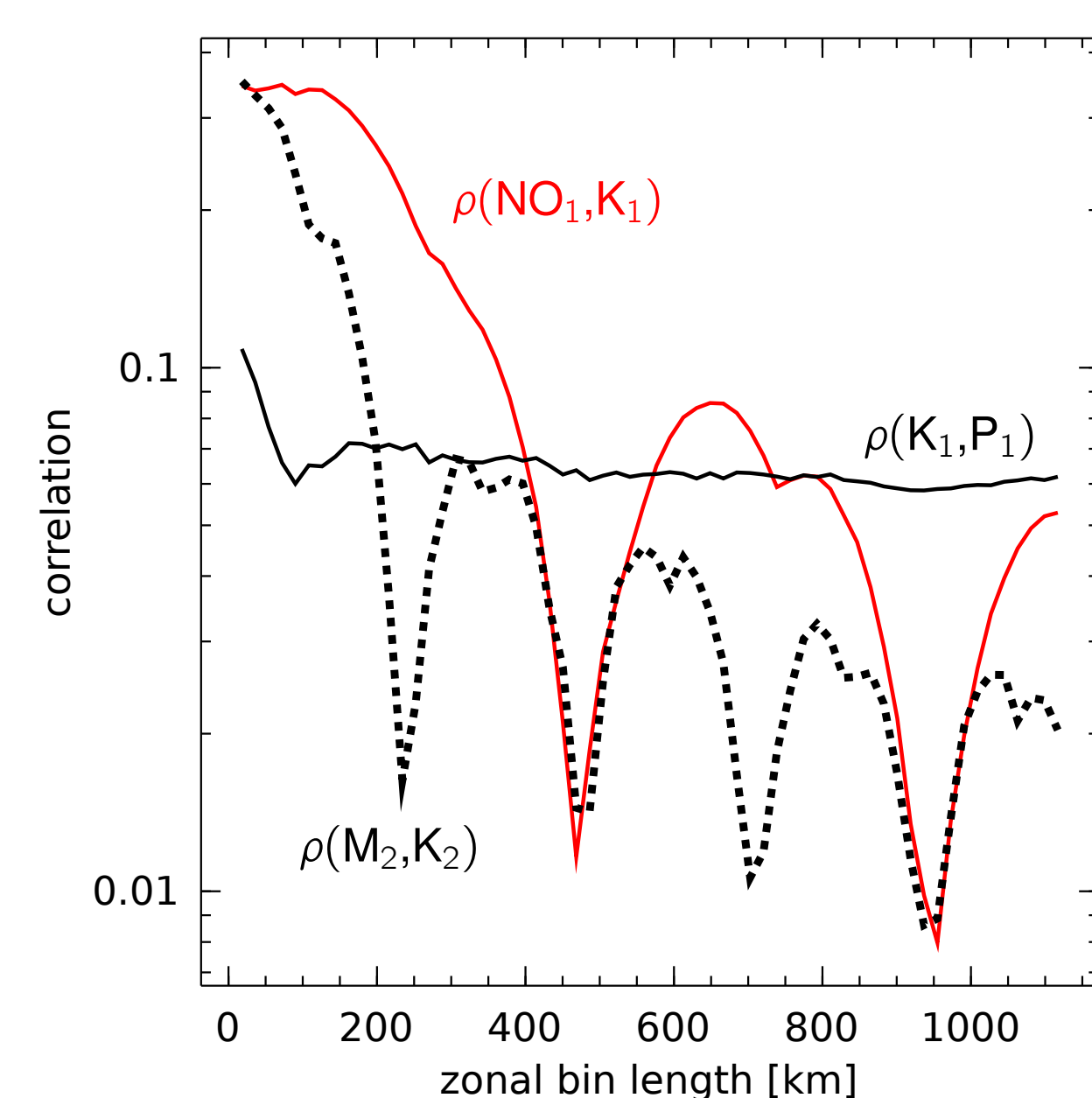


Figure 5: Theoretical error correlation at 70°S from the harmonic analysis matrix.

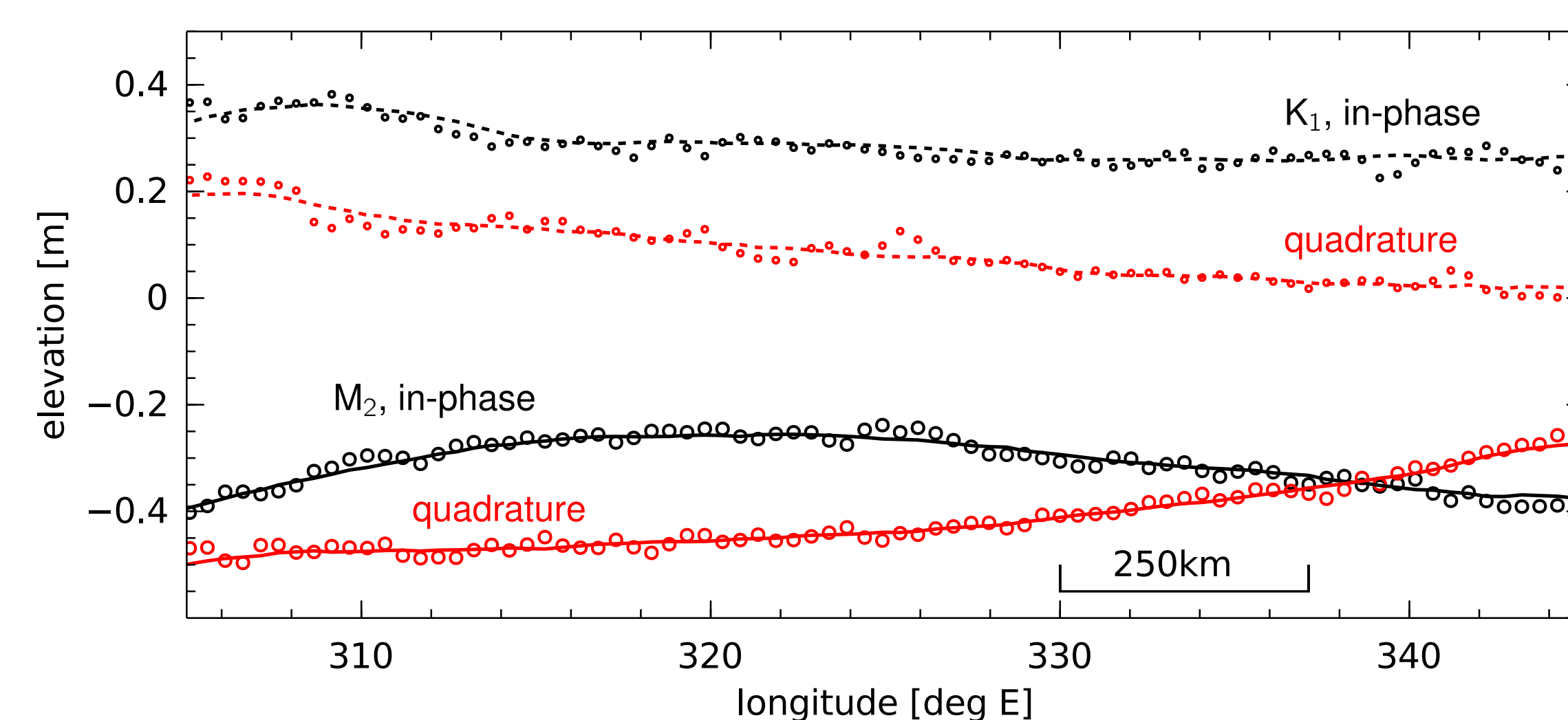


Figure 6: Tidal harmonic constants computed from CryoSat-2 data along a section at 70°S. Analysis of data within large spatial bins (lines) is needed to sample tidal phases uniformly, as compared with analysis of data within small bins (dots).

Removing the Mean Surface: LRM, SARin Mode and the Mean Surface

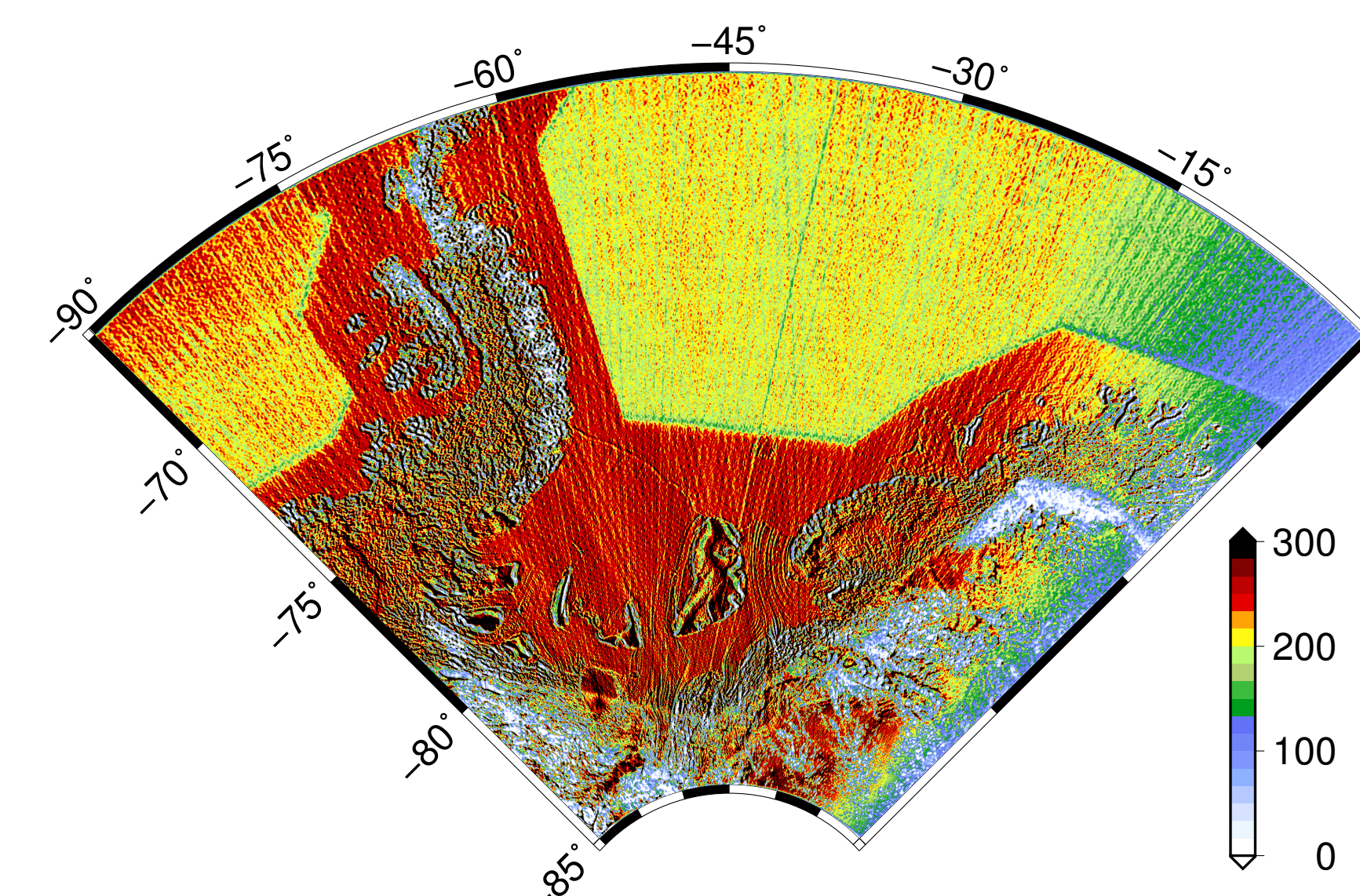


Figure 7: Number of observations per 3.5-km \times 3.5-km grid cell for Z_0 , the mean surface.

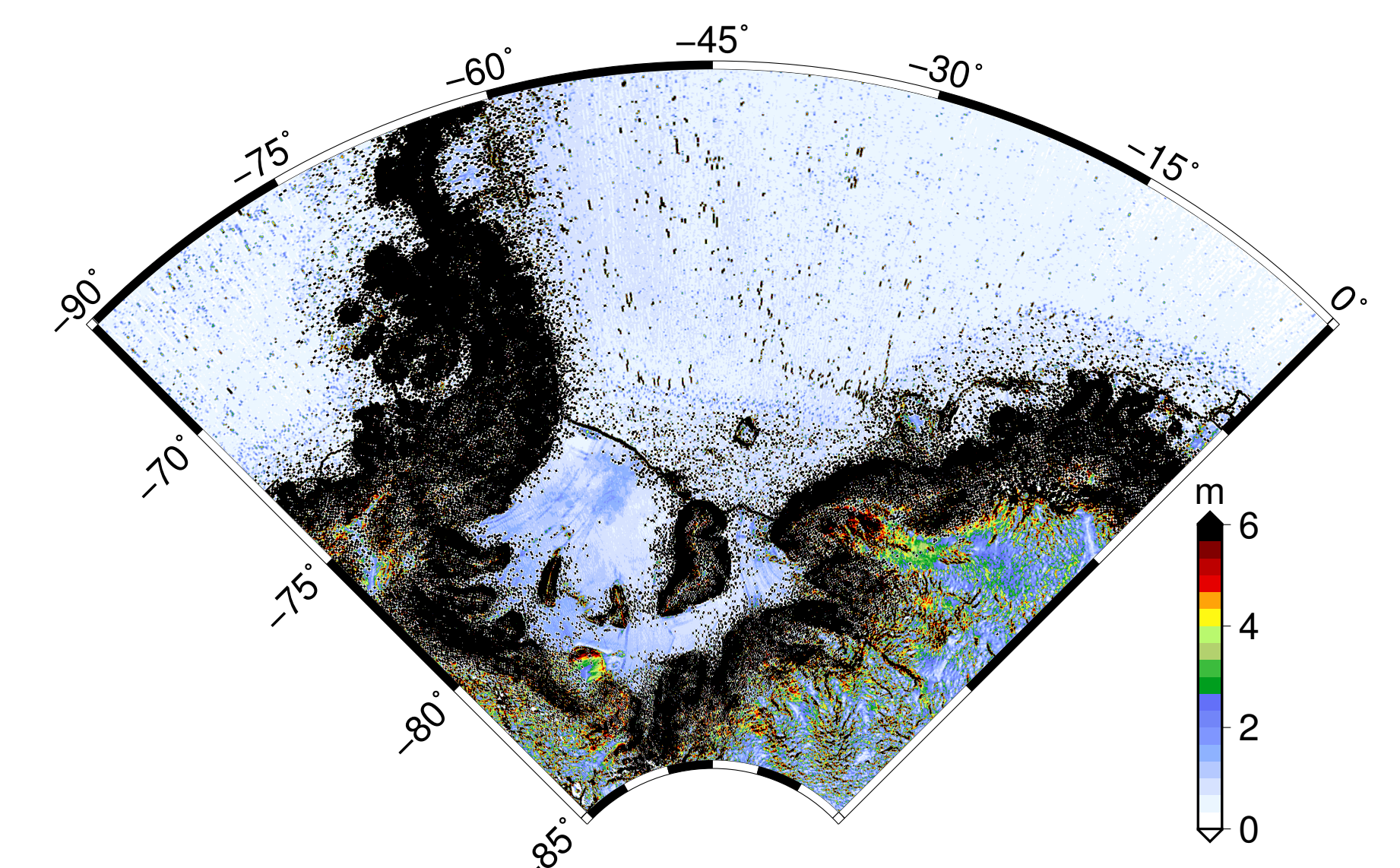


Figure 8: Standard deviation of elevation within each grid cell defining the mean surface.

Cotidal Charts

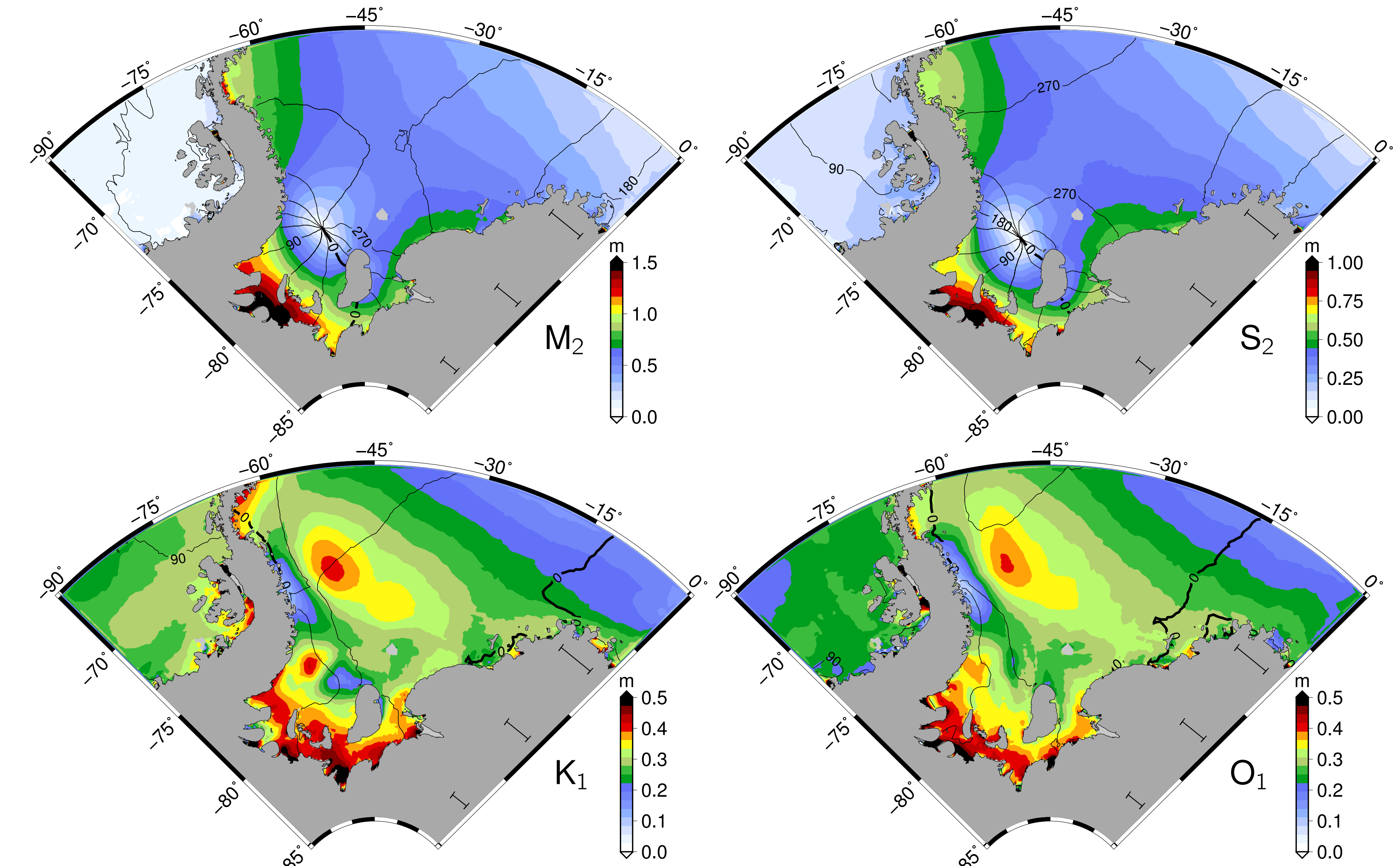


Figure 9: The four largest tides mapped from CryoSat-2 data. The amplitude is shown with the color scale, and phase lines are shown in 30° increments.

Comparisons with GOT4.10c and CATS8a Models

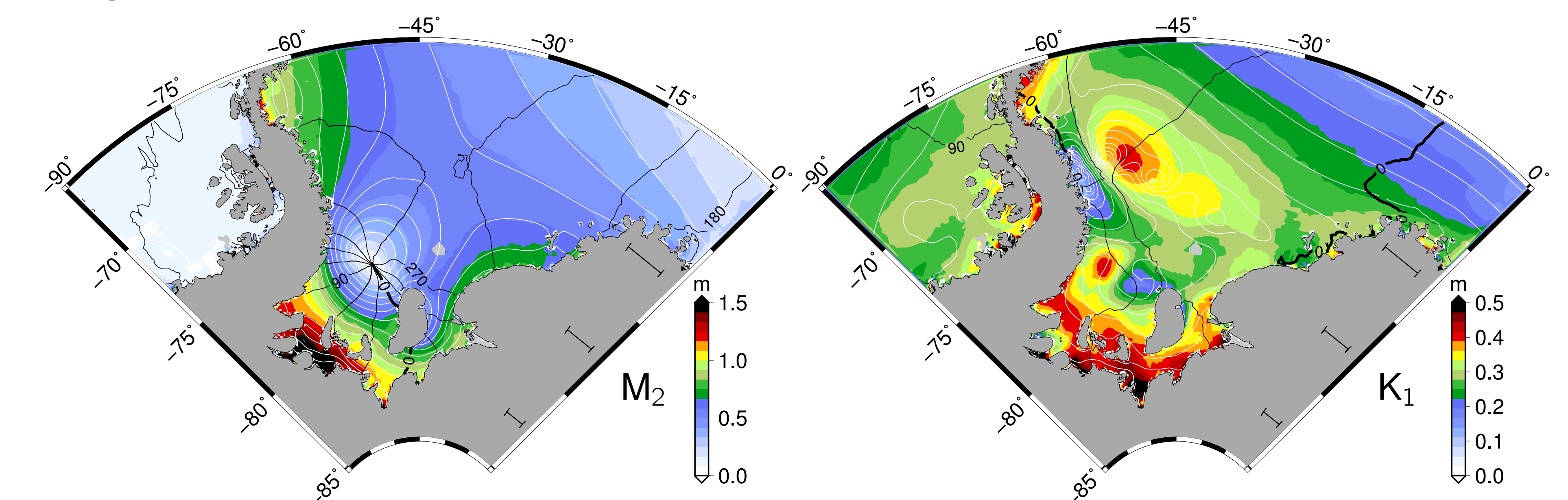


Figure 10: Comparison of the M_2 and K_1 tides from CryoSat-2 (color) versus CATS8a (white contours).

	Root-Mean Square Vector Error [cm]		
	GOT4.10c	CATS8a	CryoSat-2
M_2	4.3	4.5	3.1
S_2	8.6	7.6	6.6
N_2	1.3	2.0	1.5
K_2	2.5	2.0	4.0
K_1	4.5	2.4	2.8
O_1	5.6	1.2	2.0
P_1	1.4	1.2	1.1
Q_1	0.8	1.0	1.1

Annual Cycle of Radar Cross Section?

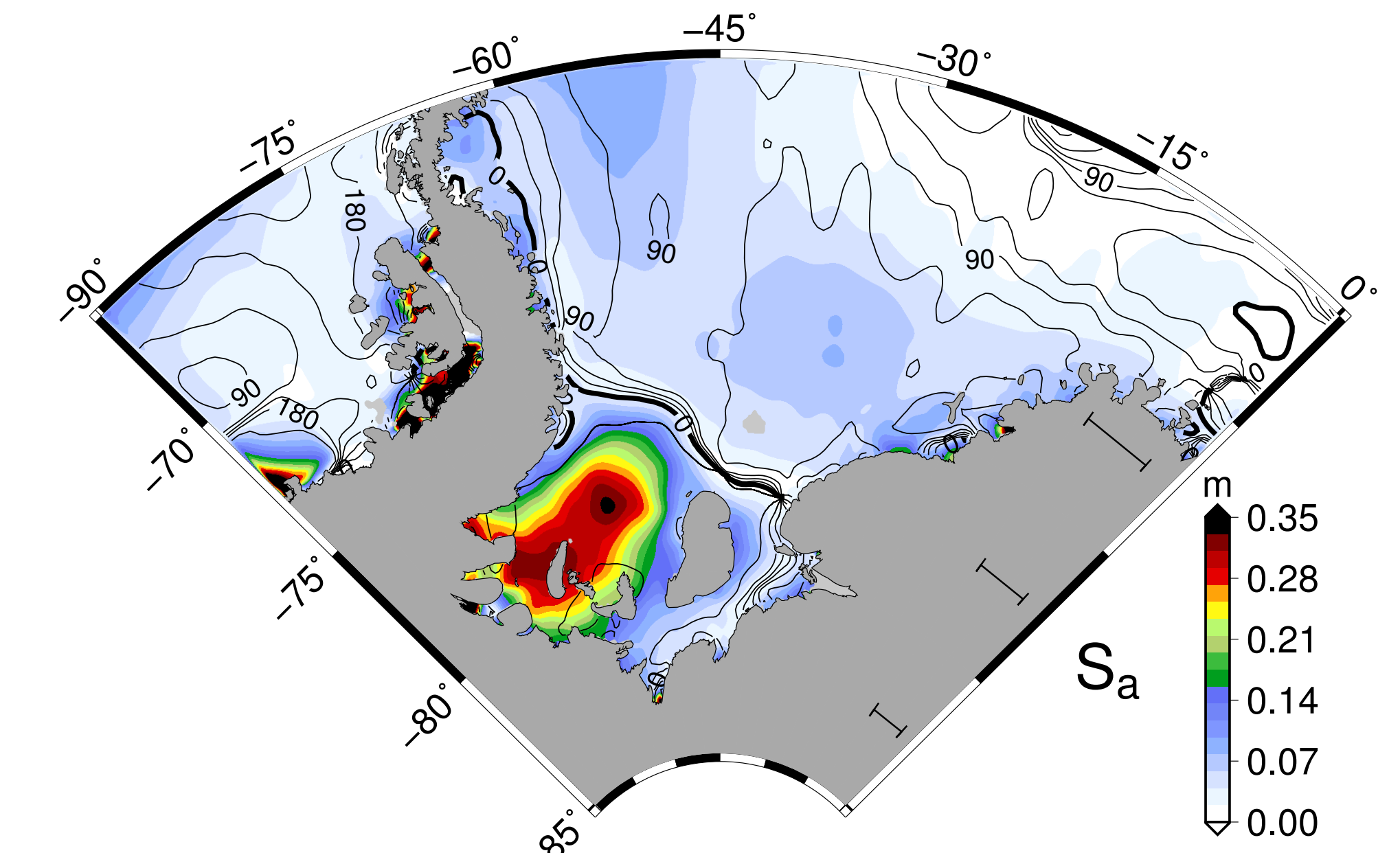


Figure 11: The annual cycle (S_a) mapped from CryoSat-2.